Estimation of steering vector errors for adaptive beamforming

Chaoying Bao and Derek Bertilone

Defence Science and Technology Organization, Australia

ABSTRACT

Steering vector errors can severely degrade the performance of adaptive beamforming. For the case of a platform-mounted array, unknown scattering from the platform can be a major source of bearing and frequency dependent errors. These errors can be estimated using a technique based on maximizing the signal-to-interference-plus-noise ratio (SINR) in the spatial spectrum computed using the minimum power distortionless response beamformer with sample matrix inverse (MPDR SMI). This technique is simple compared to some other techniques in the literature, and can be used if the noise is spatially correlated and weak interferers are present. We use simulations to show that good results are obtained if the uncertainty in the signal bearing is not too large, and interferers are sufficiently weak compared to the calibration signal.

INTRODUCTION

Adaptive beamforming (ABF) using algorithms like the minimum power distortionless response beamformer with sample matrix inverse (MPDR SMI), is widely used in sonar, radar and telecommunications (Van Trees, 2002). The MPDR SMI beamformer maximizes the signal-to-interference-plus-noise ratio (SINR) if there are no steering vector or finite-sample errors. But finite-sample errors often arise in practice because the cross-spectral matrix (CSM) is estimated using a finite quantity of data, and steering vector errors arise due to uncertainty in the array response to the signal; e.g., due to imprecise knowledge of sensor locations, unknown local scattering, or unknown propagation channel distortions such as multipath. These errors reduce the performance of ABF and can even lead to self-nulling of signals of interest (Van Trees, 2002, Vincent and Besson, 2004). For these reasons, it is common practice to make ABF more robust by applying methods such as diagonal loading (Van Trees, 2002, Li etc, 2003). Unfortunately, as the loading is increased and ABF becomes more robust to errors, the benefits of ABF over conventional beamforming are reduced. If the steering vector errors can be measured and compensated, then the level of loading required can be kept to a minimum.

This paper gives simulation results for a technique that can be used to analyse bearing and frequency dependent steering vector errors on a passive array. We refer to the phase and amplitude error at each sensor, defined relative to a nominal steering vector, as the calibration phase and calibration amplitude. We can estimate these from array recordings with targets of opportunity, using a method based on maximizing SINR in the MPDR SMI spatial spectrum (Bertilone and Bao, 2012). This method is simple compared to some other algorithms in the literature (Viberg etc, 2009, Boonstra and van der Veen, 2003, Wijnholds and van der Veen, 2009, Furguson etc, 1992, Solomon etc, 1998), and can be used if the noise is spatially correlated and weak interferers are present. Simulations show that good results are obtained if the uncertainty in the signal bearing is not too large, and interferers are sufficiently weak compared to the calibration signal. Multipath gives additional steering vector errors that are difficult to estimate and are not discussed here. Using broadband signals allows the frequency dependence of the calibration values to be obtained. The bearing dependence can be obtained using a large number of signals with a variety of fixed bearings, or alternatively, a single signal that sweeps across the required bearing range during a platform manoeuvre.

THEORY

The complex sensor outputs from an array of M sensors at frequency f are obtained from a single snapshot of data and placed in an $M \times 1$ vector $\mathbf{X}$ (Van Trees, 2002), Repeating for I snapshots of data, we form an estimate of the CSM as follows,

$$\mathbf{R} = \frac{1}{I} \sum_{i=1}^{I} \mathbf{X}^{(i)} \mathbf{X}^{(i)H}, \qquad (1)$$

where ^{H} denotes conjugate transpose. Suppose a signal arrives at the array from a bearing θ. If a large number of snapshots is available so that the finite-sample error is negligible, then

$$\mathbf{R} = \mathbf{Q} + P_S \mathbf{a}\mathbf{a}^H, \qquad (2)$$

where $\mathbf{a}$ is the true steering vector, P is the signal power, and $\mathbf{Q}$ is the CSM for interference plus noise. The elements of the true steering vector, $\mathbf{a}$, are imperfectly known in practice. We quantify the differences between the true elements and those of a nominal steering vector obtained from an idealized model, by introducing frequency and bearing dependent calibration phases, φ, and amplitudes, γ. For example, for a linear array we write,

$$a_m = \gamma_m \exp(j\varphi_m)\exp\{j2\pi(f z_m / c)\cos\theta\}, \qquad (3)$$

where z_m is the location of sensor m on the array axis, and c is wave speed. Note that the calibration phases are defined up to an additive constant, while the amplitudes are defined up to a multiplicative constant (as it is not our aim to relate sensor output to acoustic power). We choose the constants so that the mean of the phases measured across the array is zero, and the mean of the amplitudes measured across the array equals one, at each frequency and bearing.

We use a simple calibration technique based on the maximization of SINR, which applies when finite-sample error is negligible (Bertilone and Bao, 2012). It follows from the well-known optimality of MPDR beamforming (Van Trees, 2002). The output power using an assumed steering vector **b** is given by

$$P = \frac{1}{\mathbf{b}^H \mathbf{R}^{-1} \mathbf{b}} \tag{4}$$

Here the assumed steering vector, **b**, can differ from the true steering vector, **a**. Note that the SINR at the output of the beamformer when it is steered to the signal can be written as

$$\text{SINR} = \frac{P_{S+I+N} - P_{I+N}}{P_{I+N}} \tag{5}$$

where P_{S+I+N} is the output power when the signal is present together with interference and noise, and P_{I+N} is the output power when the signal is absent. The latter are given as follows,

$$P_{S+I+N} = \frac{1}{\mathbf{b}^H \mathbf{R}^{-1} \mathbf{b}} \tag{6}$$

$$P_{I+N} = \frac{1}{\mathbf{b}^H \mathbf{Q}^{-1} \mathbf{b}} \tag{7}$$

Applying Woodbury's identity (Van Trees, 2002) to Eq. (2) gives

$$\mathbf{R}^{-1} = \mathbf{Q}^{-1} - \frac{P_S \mathbf{Q}^{-1} \mathbf{a} \mathbf{a}^H \mathbf{Q}^{-1}}{1 + P_S \mathbf{a}^H \mathbf{Q}^{-1} \mathbf{a}} \tag{8}$$

so that

$$\mathbf{b}^H \mathbf{R}^{-1} \mathbf{b} = \mathbf{b}^H \mathbf{Q}^{-1} \mathbf{b} - \frac{P_S (\mathbf{b}^H \mathbf{Q}^{-1} \mathbf{a})(\mathbf{a}^H \mathbf{Q}^{-1} \mathbf{b})}{1 + P_S \mathbf{a}^H \mathbf{Q}^{-1} \mathbf{a}} \tag{9}$$

Using Eqs. (6) and (9),

$$P_{S+I+N} = \frac{1 + P_S \mathbf{a}^H \mathbf{Q}^{-1} \mathbf{a}}{\mathbf{b}^H \mathbf{Q}^{-1} \mathbf{b} + P_S \Gamma} \tag{10}$$

where

$$\Gamma = (\mathbf{b}^H \mathbf{Q}^{-1} \mathbf{b})(\mathbf{a}^H \mathbf{Q}^{-1} \mathbf{a}) - (\mathbf{b}^H \mathbf{Q}^{-1} \mathbf{a})(\mathbf{a}^H \mathbf{Q}^{-1} \mathbf{b}) \tag{11}$$

Define

$$\kappa = \frac{|\mathbf{b}^H \mathbf{Q}^{-1} \mathbf{a}|^2}{(\mathbf{b}^H \mathbf{Q}^{-1} \mathbf{b})(\mathbf{a}^H \mathbf{Q}^{-1} \mathbf{a})} \tag{12}$$

Since $\mathbf{Q}^{-1}$ is Hermitian and positive definite, the Cauchy-Schwarz inequality shows that $0 \leq \kappa \leq 1$ with $\kappa = 1$ if and only if **b** is a complex scalar times **a**. Using Eqs. (5), (7), (10) and (12),

$$\text{SINR} = \frac{P_S \kappa}{(\mathbf{a}^H \mathbf{Q}^{-1} \mathbf{a})^{-1} + P_S (1 - \kappa)} \tag{13}$$

Since SINR is maximized when $\kappa = 1$, the true steering vector can be found by varying the elements of **b** until SINR is maximized. This is the case even if the noise is spatially correlated and interferers are present. Unfortunately for a pas-

sive array, we cannot directly measure SINR so we must replace it by a proxy metric (Bertilone and Bao, 2012). This is discussed below.

Calibration algorithm

We estimate the CSM using a large number of snapshots with signal at constant bearing, and compute the MPDR SMI spatial spectrum, Eq. (4), with an assumed steering vector **b**. The bearing bin that contains the signal is assumed to be known. We replace SINR by a proxy metric $(P−μ)/μ$, where P is the power in the signal bin, and $μ$ is the mean power in a small window of bins that surrounds but excludes the signal bin and several bins on either side. The elements of **b** are varied until the global maximum of the proxy metric is found. We use a commercial optimization algorithm for this purpose. When the noise is spatially correlated, the likelihood of failure of the algorithm due to replacing SINR by a proxy can be greatly reduced if the CSM is diagonally loaded; we add $0.02 \times (\text{trace}(\mathbf{R})/M) \times \mathbf{I}$ loading, where **I** is the identity matrix.

SIMULATIONS

The aim of simulation is to evaluate the effectiveness of the algorithm under different conditions. Calibration accuracy can be quantified by computing the rms error averaged across the array, $\sigma_\varphi = \sqrt{[(1/M)\sum(\varphi_{m,true}-\varphi_{m,est})^2]}$ and $\sigma_\gamma = \sqrt{[(1/M)\sum(\gamma_{m,true}-\gamma_{m,est})^2]}$, and compare them to $\sigma_{\varphi,0}=\sqrt{[(1/M)\sum(\varphi_{m,true}-0)^2]}$ and $\sigma_{\gamma,0}=\sqrt{[(1/M)\sum(\gamma_{m,true}-1)^2]}$, the values obtained with the nominal steering vector. The quantities $100 \times \sigma_\varphi/\sigma_{\varphi,0}$ and $100 \times \sigma_\gamma/\sigma_{\gamma,0}$ give the relative rms errors after calibration, expressed as a percentage of the rms error before calibration.

We model a linear array of 16 sensors in spherically isotropic noise at frequency $f = 0.4f_d$ where $f_d = c/(2d)$ and d is sensor spacing. The noise has significant spatial correlations at this frequency (Burdic, 1991). At the start of each simulation run, calibration phases and amplitudes are assigned to each sensor at each of 201 bearings from $\cos\theta = -1$ to $+1$ by sampling uniform distributions over $(-60^o, +60^o)$ and $(1−0.5, 1+0.5)$, respectively. Noise is simulated by adding Gaussian plane waves from 201 bearings. The signal is a Gaussian plane wave arriving from a bearing located randomly within a bin-width. The signal bin is taken to be known, but the precise bearing within the bin is unknown and is resampled at each run.

Scenario 1

In this scenario, there are no interferers. The calibration signal is at $\cos\theta = 0.4$ and average input SNR per sensor varies from -3 dB to 10 dB.

Figure 1 shows results with SNR = 10 and 0 dB, respectively. Estimated vs true calibration phases and amplitudes of each sensor are plotted for 100 simulation runs. Also plotted are the distribution functions for the relative rms errors from 100 simulation runs, based on kernel estimates. The linear structure of the plots with SNR = 10 dB implies high accuracy of calibration in that case. The relative phase error is less than 6% and the relative amplitude error less than 4% for most runs. The corresponding mean errors are 2.8% and 2.2%, respectively. The accuracy of calibration with SNR = 0 dB drops a bit but is still fairly high, with the reltive phase error less than 9% and the relative amplitude error less than 15% for most runs, and the mean errors 5.7% and 9.1%, respectively.
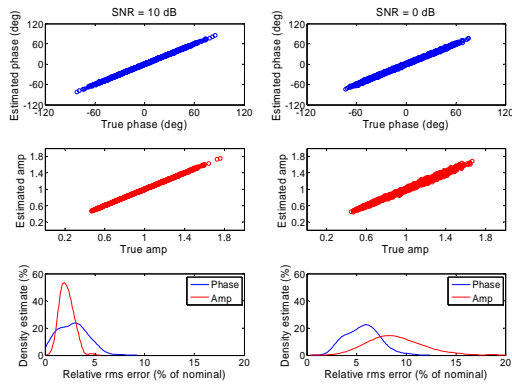
Figure 1. Estimated vs true calibration phases (top) and amplitudes (middle) of each sensor, and Kernel density estimate of distribution of relative rms errors (bottom).

Table 1 lists the mean relative rms errors with SNR = 10, 3, 0, and -3 dB, respectively. It shows that even with a relatively low SNR of -3 dB the algorithm is still able to achieve fairly high accuracy for phase calibration, which is more important for ABF.

Table 1. Mean relative rms errors

SNR (dB)	Phase error (%)	Amplitude error (%)
10	2.8	2.2
3	3.8	5.2
0	5.7	9.1
-3	12.6	21.6

Scenario 2

In this scenario, there is a single interferer. The calibration signal is at $\cos\theta = 0$ and average input SNR per sensor for the signal is 3 dB. We vary SNR of the interferer and its angle separation from the signal to evaluate the effectiveness of the algorithm.

Table 2 lists the mean relative rms errors with the interferer at $\cos\theta = 0.6$ and its SNR = 3, 0 -3, and -7 dB, respectively. It shows that in order to have reasonably high accuracy of calibration the interferer should be weaker than the calibration signal (at least 3 dB weaker in this case).

Table 2. Mean relative rms errors with single interferer at $\cos\theta = 0.6$; SNR of the signal is 3 dB.

SNR of interferer (dB)	Phase error (%)	Amplitude error (%)
3	110.4	161.7
0	10.5	21.4
-3	5.1	9.9
-7	3.7	7.5

Figure 2 plots the mean relative rms errors against the angle separation of the interferer from the calibration signal with SNR of interferer fixed at -3 and -7 dB, respectively. It shows that if the interferer is sufficiently weaker (10 dB weaker in this case) than the calibration signal, fairly high accuracy of calibration is achieved independent of the angle separation, as indicated by the blue and green solid lines. If the interferer is not sufficiently weaker (6 dB weaker in this case), reasonable accuracy of calibration is only achieveable at certain angle separations (around $\cos\theta = 0.6$ in this case), as indicated by red and black broken lines.
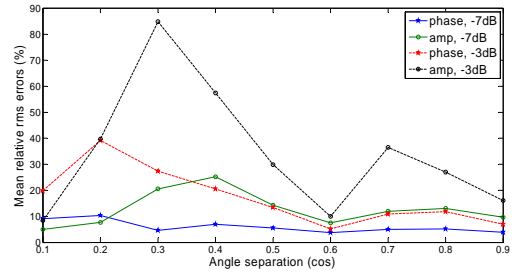

Figure 2. Mean relative rms errors against angle separation.

Scenario 3

In this scenario, there are two interferers. The calibration signal is at $\cos\theta = 0$ and average input SNR per sensor for the signal is 3 dB. We vary SNR of the interferers and their angle separation with the signal to evaluate the effectiveness of the algorithm.

Table 3 lists the mean relative rms errors with one interferer at $\cos\theta = 0.6$ and the other at $\cos\theta = -0.6$, and their SNR = 3, 0 -3, and -7 dB, respectively. Compared to the results with the single interferer listed in Table 2, the accuracy of phase calibration is quite similar when the interferers are weaker than the calibration signal, and the accuracy of amplitude calibration is a bit worse. This indicates that adding an additional interferer on the different side to the calibration signal will have a similar effect on the algorithm as that with the single interferer.

Table 3. Mean relative rms errors with two interferers at $\cos\theta = 0.6$ and -0.6; SNR of the signal is 3 dB.

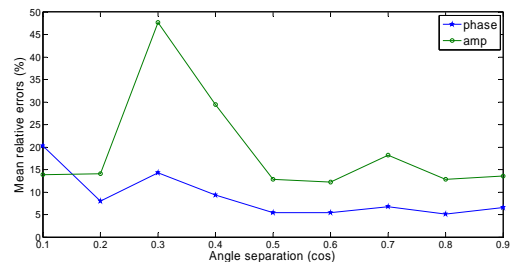| SNR of interferers (dB)	Phase error (%)	Amplitude error (%)
3	147.0	188.6
0	9.2	41.5
-3	4.6	14.4
-7	3.9	8.1

Figure 3. Mean relative rms errors against angle separation with two interferers.

Next we shall investigate the effect on the algorithm of having two interferers on the same side to the calibration signal. In the simulation, the angle separation between the two interferers is fixed to be $\cos\theta = 0.1$ and their angle separation from the calibration signal is varied. SNR of both interferers is chosen to be -7 dB. Figure 3 plots the mean relative rms errors against the angle separation of the interferers from the calibration signal obtained from the simulation. Compared to the case with single interferer (blue and green solid lines in Figure 2), accuracy for both phase and amplitude calibration is reduced noticeably when the angle separation is smaller than 0.4. To increase accuracy of calibration, the SNRs of the interferers need to be reduced further.

CONCLUSION

Steering vector errors can severely degrade the performance of ABF. For the case of a platform-mounted array, unknown scattering from the platform can be a major source of bearing and frequency dependent errors. These errors can be estimated using a technique based on maximizing the SINR in the spatial spectrum computed using MPDR SMI. We have used simulations to show that the technigue is effective if the uncertainty in signal bearing is small, and interferers are sufficiently weak compared to the calibration signal.

REFERENCES

Bertilone, D & Bao, C 2012 'Estimation of steering vector errors due to local scatter on a passive hull-mounted array,' *JASA Express Letters*, to be submitted.

Boonstra, A & van der Veen, A 2003, 'Gain calibration methods for radio telescope arrays,' *IEEE Trans. Signal Proc.*, **51**, pp. 25-38.

Burdic, WS 1991, *Underwater Acoustic System Analysis*, 2nd Ed., Prentice Hall, Englewood Cliffs, NJ.

Ferguson, B, Gray, D and Riley, J 1992 "Comparison of sharpness and eigenvector methods for towed array shape estimation", *JASA,* **91(3)**, pp.1565

Li, J, Stoica, P & Wang, Z 2003 'On robust Capon beamforming and diagonal loading,' *IEEE Trans. Signal Proc.*, **51**, pp. 1702-1715.

Pease, MC 1965, *Methods of Matrix Algebra*, Academic Press, New York.

Solomon, D, Gray, D, Abramovich, Y and Anderson, S 1998 "Over-the-horizon Radar Array Calibration using Echoes from Ionised Meteor Trails", *IEE Proc.– Radar Sonar Navig.*, **145(3)**, pp. 173-180.

Van Trees, HL 2002, *Optimum Array Processing, Part IV of Detection, Estimation and Modulation Theory,* Wiley-Interscience, New York.

Viberg, M, Lanne, M & Lundgren, A 2009 'Calibration in array processing,' in *Classical and Modern Direction-of-Arrival Estimation*, T. Tuncer and B. Friedlander, Eds., Academic Press, Burlington, MA.

Vincent, F & Besson, O 2004 'Steering vector errors and diagonal loading,' *IEE Proc.– Radar Sonar Navig.*, **151**, pp. 337-343.

Wijnholds, SJ & van der Veen, A 2009, 'Multisource self-calibration for sensor arrays,' *IEEE Trans. Signal Proc.*, **57**, pp. 3512-3522.